

HEAT EFFICIENCY OF GEOTHERMAL ELECTRICAL STATIONS WITH HYDROSTEAM TURBINES

Vladimir A. Barilovich and Youry A. Smirnov

Saint Petersburg State Technical University, Polytechnicheskaya 29, 195251, St.Petersburg, Russia

Key words: hydrosteam turbines, analysis, experience

ABSTRACT

A thermodynamic analysis of world geothermal electrical generating stations (GHES) shows the significant losses of flow exergy occur in separators or flash vessels where thermal water is flashed and then separated to produce dry saturated steam for conventional intermediate steam turbines. These losses can be greatly reduced by using hydrosteam flashing flow turbines instead of conventional separated steam system, as shown in Barilovich (1982,1993), Barilovich *et al.*,(1985,1998). In spite of low internal relative heat efficiency (presently $\hbar_{oi}=0.32 \dots 0.42$) such turbines, when used in GHES under low dryness degree of thermal water ($x<0.2$) at temperature of 430...450K can raise the actual power of the station by 5...20%.

1. INTRODUCTION

The work consists of thermodynamic analysis of total flow GHES with axial-flow and Pelton turbines having optimized thermal parameters and a comparison of suggested heat schemes to conventional ones using separators. The basic concept of calculations of axial-flow and Pelton turbines are considered and the results of author's experimental investigations of Laval nozzles with steam generating lattices, high speed wall fluid flow in rectangle duct and 100 kW active axial-flow hydrosteam turbine (HST) working at overheated water, are presented. Use of Laval nozzles with steam generating lattices and velocity factors of 0.85...0.87 developed in St.Petersburg Technical University (formerly Leningrad Polytechnic Institute) will allow the creation of hydrosteam turbines with $\hbar_{oi}=0.5 \dots 0.55$ that provide still greater increase in GHES efficiency.

2. THERMODYNAMIC ANALYSIS OF GHES WITH HST

Let's consider two possible schemes of GHES with HST. First scheme (Fig.1) includes two one-stage axial active turbines, the second one (Fig.2) consists of one axial and one Pelton turbine with jet condenser-mixer. The systems of equations for calculation of both schemes are presented below.

Common equations for both schemes are:

$$\begin{aligned} i_{2s} &= i'_2 + \left(\frac{\tilde{\eta}_1}{T_1} + c_p \ln \frac{T_1}{T_2} \right) T_2; \\ x_{2a,ST} &= (1 - \hbar_{oi}^{ST}) (i'_1 - i_{2s}) / \tilde{r}_2 + x_{2s,ST}; \\ x_{2s,ST} &= \left(\frac{\eta_1}{T_1} + c_p \ln \frac{T_1}{T_2} \right) T_2 / \tilde{r}_2; \quad G_{v1} = G_{mix} x_1; \\ x_{2a} &= i''_1 - (i'' - i_{2s}) \hbar_{oi}^{ST}; \quad i_{2a} = i''_1 - (i'' - i_{2s}) \hbar_{oi}^{ST}; \\ x_{2a} &= s'_1 + (x_{2a,ST} - x_{2s,ST}) \tilde{r}_2 / T_2; \end{aligned}$$

$$\begin{aligned} x_2 &= c_p \left(T_2 \ln \frac{T_1}{T_2} + T_1 \left(1 - T_2 \left(1 + \ln \frac{T_1}{T_2} \right) / T_1 \right) \left(1 - \hbar_{oi}^{HST} \right) \right) / \tilde{r}_2; \\ N_{HST1} &= (1 - x_1) G_{mix} \hbar_{oi}^{HST} c_p \left(T_1 - T_2 \left(1 + \ln \frac{T_1}{T_2} \right) \right) \end{aligned}$$

Equations for scheme No.1 are:

$$\begin{aligned} G_{v2} &= G_{mix} (1 - x_1) x_2; \quad s_{mix2} = (s_{2a} G_{v1} + s''_2 G_{v2}) / (G_{v1} + G_{v2}); \\ i_{mix2} &= (i_{2a} G_{v1} + i''_2 G_{v2}) / (G_{v1} + G_{v2}); \\ x_3 &= c_p T_3 \ln \frac{T_2}{T_3} + T_2 \left(1 - T_3 \left(1 + \ln \frac{T_2}{T_3} \right) / T_2 \left(1 - \hbar_{oi}^{HST} \right) \right) / \tilde{r}_3; \\ x_{3s,ST} &= (s_{mix2} - s'_3) T_3 / \tilde{r}_3; \quad G_{v3} = G_{mix} (1 - x_1) (1 - x_2) x_3; \\ G_{f3} &= G_{mix} (1 - x_1) (1 - x_2) (1 - x_3); \\ N_{HST2} &= (1 - x_1) (1 - x_2) G_{mix} \hbar_{oi}^{HST} c_p \left(T_2 - T_3 \left(1 + \ln \frac{T_2}{T_3} \right) \right); \\ i_{3s} &= i'_{3s} + \left(s_{mix2} - c_p \ln \frac{T_3}{273} \right) T_3; \end{aligned}$$

$$\begin{aligned} i_{3a} &= i_{mix2} - (i_{mix2} - i_{3s}) \hbar_{oi}^{ST}; \\ i_{mix3} &= (i_{3a} (G_{v1} + G_{v2}) + i''_3 G_{v3}) / (G_{v1} + G_{v2} + G_{v3}); \\ s'_3 &= s'(T_3) + \tilde{r}_3 / T_3; \quad s_{3a} = s_{mix2} + (i_{3a} - i_{3s}) / T_3; \\ s_{mix3} &= (s_{3a} (G_{v1} + G_{v2}) + s''_3 G_{v3}) / (G_{v1} + G_{v2} + G_{v3}); \\ i_{\tilde{n}} &= i'_{\tilde{n}} + \left(s_{mix3} - c_p \ln \frac{T_{\tilde{n}}}{273} \right) T_{\tilde{n}}; \\ i_{\tilde{n}} &= i_{mix3} - (i_{mix3} - i_{\tilde{n}}) \hbar_{oi}^{ST}; \quad x_{\tilde{n}} = (i_{\tilde{n}} - i'_{\tilde{n}}) / \tilde{r}_{\tilde{n}}; \\ i_6 &= \left(\left(i'_{\tilde{n}} + (p_4 - p_{\tilde{n}}) \mathbf{n}'_{\tilde{n}} / \hbar_{oi}^p \right) (G_{v1} + G_{v2} + G_{v3}) + G_{f3} i_5 \right) / (G_{v1} + G_{v2} + G_{v3} + G_{f3}); \\ i_7 &= i_6 + (p_7 - p_6) \mathbf{n}_6 / \hbar_{oi}^p; \\ N_{ST} &= (i''_1 - i_{2a}) G_{v1} + (i_{mix2} - i_{3a}) (G_{v1} + G_{v2}) + (i_{mix2} - i_{ca}) (G_{v1} + G_{v2} + G_{v3}); \\ N_{P1} &= (p_5 - p_3) \mathbf{n}'_3 G_{f3} / \hbar_{oi}^p; \\ N_{P2} &= (p_4 - p_c) \mathbf{n}_c (G_{v1} + G_{v2} + G_{v3}) / \hbar_{oi}^p; \\ N_{P3} &= (p_7 - p_6) \mathbf{n}_6 G_{mix} / \hbar_{oi}^p; \\ N_{GEO} &= N_{ST} + N_{HST1} + N_{HST2} - N_{P1} - N_{P2} - N_{P3}; \\ t_7 &= 1,148 + 0,24685 \cdot 10^{-3} \cdot i_7 - 1,27 \cdot 10^{-5} (i_7 \cdot 10^{-3})^2; \\ i_{mix1} &= i'_1 (1 - x_1) + i''_1 x_1; \quad s_{mix1} = s'_1 (1 - x_1) + s''_1 x_1; \\ \hbar_i &= N_{GEO} / [(i_{mix1} - i_7) G_{mix}]; \\ \hbar_{ex} &= N_{GEO} / [G_{mix} (i_{mix1} - i_e) (s_{mix1} - s_e)], \text{ where} \end{aligned}$$

c_p - specific heat capacity of fluid, G -expenditure, i,s -specific enthalpy and entropy, N -capacity, \tilde{r} -specific heat of evaporation, p -pressure, T -temperature, v -specific volume, x -dryness degree of steam, \hbar_i , \hbar_{oi} , \hbar_{ex} -absolute internal, relative internal and exergy efficiency, subscripts: 1...7,c,p-

see Fig.1, a - actual, f - fluid, e - environment, s - isoentropic, v - vapor, mix - hydrosteam mixture.

The system of equations for scheme No. 2 is:

$$\begin{aligned}
 i_{cs} &= i'_c + \left(s_{mix2} - c_p \ln \frac{T_c}{273} \right) f_c; \\
 i_{ca} &= i_{mix2} - (i_{mix2} - i_{ca}) \mathbf{h}_{oi}^{ST}; \\
 N_{ST} &= (i''_1 - i_{2a}) G_{v1} + (i_{mix2} - i_{ca}) (G_{v1} + G_{v2}); \\
 G_n &= (1 - x_1)(1 - x_2) G_{mix}; x_3 = \left(c_p T_3 \ln \frac{T_2}{T_3} \right) \tilde{r}_3; \\
 G_w &= G_n x_3 \tilde{r}_3 / \left[\epsilon_p (T_3 - T_e - \Delta T_u) \right]; \\
 \Delta i_s &= c_p \left(T_2 - T_3 - T_3 \ln \frac{T_2}{T_3} \right); c_{ns} = \sqrt{2\Delta i_s}; c_{na} = \mathbf{j}_1 c_{ns}; \\
 N_{P3} &= p_e G_w (\mathbf{p}_p - 1) / \left(\mathbf{h}_{oi}^p \mathbf{r}_w \right); \mathbf{p}_p = p_p / p_e; \\
 p_p &= p_e + \Delta p_p; \Delta p_p = N_{P3} \mathbf{r}_w \mathbf{h}_{oi}^p / G_w; \\
 c_{wa} &= \mathbf{j}_2 \sqrt{2(p_p - p_3) / \mathbf{r}_w}; \\
 c_{mix} &= (c_{na} G_n + c_{wa} G_w) / (G_n + G_w); G_{HST2} = G_n + G_w; \\
 N_{P1} &= G_{HST2} (p_5 - p_3) \mathbf{v}_3' / \mathbf{h}_{oi}^{P1}; \\
 N_{HST2} &= u (c_{mix} - u) G_{HST2} (1 - \mathbf{y} \cos \mathbf{b}); u = 0.46 c_{mix}; \\
 N_{P2} &= (p_4 - p_c) \mathbf{v}_c (G_{v1} + G_{v2}) / \mathbf{h}_{oi}^{P2}; \\
 N_{P4} &= (p_7 - p_6) \mathbf{v}_6 (G_{mix} + G_w) / \mathbf{h}_{oi}^{P4}; \\
 N_{GEO} &= N_{ST} + N_{HST1} + N_{HST2} - N_{P1} - N_{P2} - N_{P3} - N_{P4},
 \end{aligned}$$

where c - absolute flow velocity, u - circumferential rotor velocity at mean diameter, ΔT_u - underheating of cold water to saturation temp., \mathbf{b} -flow angle in relative moving at exit from scoop, \mathbf{r} -density, $\mathbf{j}_1, \mathbf{j}_2$, \mathbf{y} -velocity coeff. of active and passive nozzle and working wheel respectively; subscripts: n -nozzle, w -water.

The results of calculations are presented in Table 1. It was estimated that the pressure of returned water is equal to the that of thermal mixture at GHES entry, a temperature is not less than 343K, hydraulic losses are neglected, the pressure in steam turbine condenser is equal to 0.01 MPa. Table 1 also presents optimal values of relative temperatures t_2/t_{mix} and t_3/t_{mix} at HST exit giving a maximum of circle useful capacity. Some advantage of scheme with one ST and two HST in comparison to scheme of ST, HST and Pelton turbines decreases while x_{mix} increases. Creating GHES of one ST and one Pelton HST with condenser-mixer is unreasonable for its low efficiency due to high exergy losses in Pelton HST.

Using of axial HST in GHES raises a question on maximal capacity of HST. As the working medium in HST is almost saturated fluid, the heat drop is about ten times less than in steam turbine at the same temperature interval, so a considerable capacity may be reached by increasing of turbine hot water flow. The greater HST pressure drop, the greater specific work, and the less flow capacity of the turbine because of decreasing in steam density. Thus, there is back pressure at which a capacity of single-row axial active turbine (at given D_m/h_b , where D_m - diameter of working wheel at mean blade height, h_b - blade height, and rotor angle velocity

w) gets maximal value. The HST capacity at known back pressure $p_1 = f(T_1)$ is defined by formula

$$\begin{aligned}
 N_{HST} &= \frac{8p\sqrt{2}(u/c_{1t})^2 \mathbf{j}_{n1}^2 \mathbf{h}_{oi} \overline{(\mathbf{r}_{c1})}_a}{(D_m/h_b) \mathbf{w}^2} \times \\
 &\times \frac{\left\{ \frac{c}{c_p} \left[T_0 - T_1 \left(1 + \ln \frac{T_0^*}{T_1} \right) \right] \right\}^{5/2} \sin \mathbf{a}_1}{\left[v_1' + (v'' - v')_1 \frac{c}{c_p} T_1 \ln \left(\frac{T_0^*}{T_1} \right) \right]^{1/2}},
 \end{aligned}$$

where c_{1t} -theoretical absolute velocity at exit from nozzle apparatus, \mathbf{a}_1 - angle between velocity vectors u and c_{1t} , T_0^* - temperature of hot water at entry to turbine, $\left(\overline{\mathbf{r}_c} \right)_a = \frac{(\mathbf{r}_c)_{1a}}{(\mathbf{r}_c)_{1t}} = 1.3$ for HST nozzle apparatus with steam generating lattices. According to calculations, the HST capacity at $p_0^* = 0.6$ MPa, $T_0^* = 428$ K, $p_{lopt} = 0.0173$ MPa is equal to 21.8 MW ($n=500$ r.p.m., $D_m/h_b = 7$). The unit with $D_m/h_b = 5$ has the capacity up to 30.5 MW. Such a powerful HST should have vertical shaft and be similar to construction of hydraulic turbines. The Pelton turbine with jet condenser-mixer included in GHES permits to get capacity up to 50 MW in single unit. In this case, however, a pump in cold water line should be added to reduce the shock losses in mixing camera (MC).

3. THE PREDICTION OF FLASHING FLOW LAVAL NOZZLE WITH STEAM GENERATING LATTICE

Using of flashing flow as working medium in turbines and jet units raises a task of determining the maximum possible degree of conversion of fluid heat into kinetic energy of flow. The experiments with Laval nozzles of conventional form working at almost saturated hot water have shown that at low initial pressure ($p_0^* = 0.4...0.8$ MPa) the velocity coefficient is small ($\mathbf{j} \leq 0.7$) because of significant thermal and mechanical non-equilibrium of flow. Mounting of the steam generating lattice (a disk with cylindrical holes of $d=0.8...0.9$ mm, $l/d=6$), into the nozzle leads to formation of fine-dispersed flow structure and to growth of nozzle efficiency. The idea of nozzle with lattice belongs to Prof. V.A.Zysin (1976). Prof. Barilovich *et al.*, (1987) have created a nozzle with steam generating lattice having a velocity coefficient $\mathbf{j}_n = 0.85...0.87$ (see Fig.3). Such a high \mathbf{j}_n received at nozzle working at overheated water under low initial pressure is probably close to its limiting value and correlates with experiments of O.Frenzl (1956) with Laval nozzles of conventional form under high initial pressure. So, at $p_0^* = 4$ MPa he has obtained $\mathbf{j}_n = 0.87$. Since a nozzle apparatus of high-effective HST should consist of group of Laval nozzles with steam generating lattices, let's consider the basic concepts of numerical calculation of such nozzles. The less number of holes in lattice n_h , the higher lattice pressure drop, so at definite pressure drop a flow with density less than boundary one may be received and a process may be

described by conservation equations for droplet-vapor structure of flow. The physical values after the lattice at given droplet size are defined using the conservation equations of flow enthalpy and expenditure. Solving the system of equations, we get a formula

$$\begin{aligned} \frac{dp}{dz} = & \left\{ \frac{3}{4} c_x \mathbf{r}_v c_v \frac{f_d}{D_d} \left(\frac{c_v}{c_d} - 1 \right) \frac{c_v}{c_d} - 1 \left(\left(\frac{c_d}{c_v} \right)^2 - \frac{\mathbf{r}_v}{\mathbf{r}_d} \right) + \right. \\ & + 6 \left(2 - \frac{c_d}{c_v} - \frac{c_v \mathbf{r}_v}{c_d \mathbf{r}_d} \right) \frac{f_d j_{d-v}}{D_d} + c_f \frac{c_v \mathbf{r}_v}{2} \mathbf{p} D_n - c_v \mathbf{r}_v \frac{dF_n}{dz} \left. \right\} \times \\ & \times c_v \left/ \left[\left(\frac{dp}{d\mathbf{r}_v} - \left(\frac{c_v}{c_d} \right)^3 \left(\frac{\mathbf{r}_v}{\mathbf{r}_d} \right)^2 \frac{G_d}{G_v} - 1 \right) f_v \right] \right\} \end{aligned}$$

(c_x -resistance coeff. of droplet, c_f - friction coeff. F_n -cross-section area, j -specific mass flux; subscripts: d -droplet), in which a role of each effect (friction, mass transfer and channel geometry) is clearly seen. The formula at isentropic flow and droplet absence transforms to well known

$$\frac{dp}{dz} = -kM^2 \rho (dF_n/dz) / \left[(M^2 - 1) F_n \right].$$

The obtained expression of pressure gradient dp/dz allows to solve a direct task (with known nozzle cross section dependence on longitudinal coordinate $F_n = f(z)$) for flow movement in the nozzle. Besides, we have:

$$\begin{aligned} \frac{dc_d}{dz} = & \frac{3}{4} c_x \frac{\mathbf{r}_v}{\mathbf{r}_d} \frac{c_d}{D_d} \left(\frac{c_v}{c_d} - 1 \right) \frac{c_v}{c_d} - 1 \left| - \frac{1}{\mathbf{r}_d c_d} \frac{dp}{dz} \right. \\ \frac{dc_v}{dz} = & -\frac{3}{4} c_x \frac{f_d}{D_d} \frac{c_d^2}{c_v f_v} \left(\frac{c_v}{c_d} - 1 \right) \frac{c_v}{c_d} - 1 \left| - \right. \\ & - \frac{1}{\mathbf{r}_v c_v} \frac{dp}{dz} - \frac{c_f c_v \mathbf{p} D_n}{2 f_v} - \frac{6(c_v - c_d) f_d j_{d-v}}{c_v \mathbf{r}_v f_v D_d}, \end{aligned}$$

$$dG_v/dz = \Delta j \mathbf{p} D_d^2 F_n n_V = 6 \Delta j G_d / (D_d c_d \mathbf{r}_d),$$

$$dD_d/dz = -2 \Delta j / (c_d \mathbf{r}_d), \quad dx/dz = \Delta j \mathbf{p} D_d^2 n_V F_n / G,$$

$$dT_d/dz = -\frac{6}{c_{pd} \mathbf{r}_d D_d c_d} (a(T_d - T_v) + \tilde{r} \Delta j),$$

where $n_V = n / c_d / F_n$ -volume droplet concentration,

$$n = 6 G_d / (\mathbf{p} D_d^3 \mathbf{r}_d) - \text{droplet flux, s}^{-1},$$

$$\Delta j = j_{d-v} - j_{v-d} = \frac{c}{\sqrt{2} \mathbf{p} \tilde{R}_v} \left(\frac{p(T_d)}{\sqrt{T_d}} - \frac{p}{\sqrt{T}} \right), \quad c = \frac{35}{p^{0.56}},$$

$$T = f(p); \quad c_f = f(\text{Re}_v); \quad c_x = f(\text{Re}_d); \quad G_d = G - G_v;$$

$$f_d = G_d / (\mathbf{r}_d c_d); \quad f_v = F_n - f_d.$$

4. PREDICTING OF WORKING WHEEL CHANNEL OF SINGLE-ROW AXIAL HST

The continuity equation of steam flow in Euler form at presence of mass sources is:

$$\frac{d}{d\mathbf{j}} (w_v \mathbf{j} r_v \mathbf{j}_v) = \mathbf{p} D_d^2 \Delta j n_V r,$$

where \mathbf{j}_v - true vapor content, r -current channel radius. After differentiating of above equation we get

$$\frac{dw_v \mathbf{j}}{d\mathbf{j}} = \frac{\mathbf{p} D_d^2 \Delta j n_V r}{\mathbf{r}_v \mathbf{j}_v} - \frac{w_v \mathbf{j}}{\mathbf{r}_v} \frac{d\mathbf{r}_v}{dp} \frac{dp}{d\mathbf{j}} - \frac{w_v \mathbf{j}}{\mathbf{j}_v} \frac{d\mathbf{j}_v}{d\mathbf{j}}.$$

To exclude $d\mathbf{j}_v / d\mathbf{j}$ let's write a relationship between volume portions of vapor \mathbf{b}_v and droplets \mathbf{g}_d in a cell

$$\mathbf{b}_v = 1 - \mathbf{g}_d = 1 - \mathbf{p} D_d^3 n_V / 6, \text{ so } \frac{d\mathbf{b}_v}{d\mathbf{j}} = -\frac{\mathbf{p} D_d^2}{2} n_V \frac{dD_d}{d\mathbf{j}},$$

$$\text{but } \frac{dD_d}{d\mathbf{j}} = -\frac{2 \Delta j r}{\mathbf{r}_v w_d \mathbf{j}}, \text{ and } \frac{d\mathbf{b}_v}{d\mathbf{j}} = -\frac{\mathbf{p} D_d^2}{\mathbf{r}_d w_d \mathbf{j}} \Delta j n_V r.$$

It may be shown that $\mathbf{b}_v = (\mathbf{j}_v + \mathbf{j}_v(\mathbf{j} + d\mathbf{j})) / 2$, and $d\mathbf{b}_v = d\mathbf{j}_v + d\mathbf{j}_v^2 / 2$ or $d\mathbf{b}_v \approx d\mathbf{j}_v$, so the continuity equation becomes as follows:

$$\frac{dw_v \mathbf{j}}{d\mathbf{j}} = \frac{\mathbf{p} D_d^2 \Delta j n_V r}{\mathbf{j}_v} \left(\frac{1}{\mathbf{r}_v} - \frac{w_v \mathbf{j}}{w_d \mathbf{j} \mathbf{r}_d} \right) - \frac{w_v \mathbf{j}}{\mathbf{r}_v} \frac{d\mathbf{r}_v}{dp} \frac{dp}{d\mathbf{j}}.$$

In our case $\partial w_v \mathbf{j} / \partial t = 0$, $w_{vr} = 0$, $dr/d\mathbf{j} = 0$, so

$$\frac{dp}{d\mathbf{j}} = \left(\frac{\partial p}{\partial r} \right)_j \frac{dr}{d\mathbf{j}} + \left(\frac{\partial p}{\partial \mathbf{j}} \right)_r = \left(\frac{\partial p}{\partial \mathbf{j}} \right)_r.$$

The vapor flow momentum equation may be written as:

$$\begin{aligned} \frac{dw_v \mathbf{j}}{d\mathbf{j}} = & -\frac{1}{w_v \mathbf{j} \mathbf{r}_v} \frac{dp}{d\mathbf{j}} - c_x \frac{\mathbf{p} D_d^2}{8 \mathbf{j}_v} \left(1 - \frac{w_d \mathbf{j}}{w_v \mathbf{j}} \right) \Delta w n_V - \\ & - \left(1 - \frac{w_d \mathbf{j}}{w_v \mathbf{j}} \right) \frac{\mathbf{p} D_d^2 n_V \Delta j r}{\mathbf{r}_v \mathbf{j}_v}, \end{aligned}$$

$$\text{where } \Delta w = \sqrt{(w_{vr} - w_{dr})^2 + (w_v \mathbf{j} - w_d \mathbf{j})^2}.$$

Equating $dw_v \mathbf{j} / d\mathbf{j}$ from continuity and momentum equations, we define an angular pressure gradient along the channel:

$$\begin{aligned} \frac{dp}{d\mathbf{j}} = & \frac{\mathbf{r}_v w_v \mathbf{j}}{\left(\frac{w_v \mathbf{j}}{w_d \mathbf{j}} - 1 \right)} \left\{ c_x \frac{\mathbf{p} D_d^2}{8 \mathbf{j}_v} \left(1 - \frac{w_d \mathbf{j}}{w_v \mathbf{j}} \right) \Delta w n_V + \right. \\ & \left. + \left[\left(1 - \frac{w_d \mathbf{j}}{w_v \mathbf{j}} \right) + \left(1 - \frac{w_v \mathbf{j}}{w_d \mathbf{j}} \right) \frac{\mathbf{p} D_d^2 n_V \Delta j r}{\mathbf{r}_v \mathbf{j}_v} \right] \right\}. \end{aligned}$$

The momentum equation for evaporating droplet in coordinate form (taking in account a streamline equation $dr/w_{dr} = r d\mathbf{j} / w_d \mathbf{j}$ at $w_{vr} = 0$) is:

$$\frac{dw_d \mathbf{j}}{d\mathbf{j}} = \tilde{F} \left(\frac{w_v \mathbf{j}}{w_d \mathbf{j}} - 1 \right) r - w_{dr}, \quad \frac{dw_{dr}}{d\mathbf{j}} = w_d \mathbf{j} - \tilde{F} \frac{w_{dr}}{w_d \mathbf{j}} r,$$

$$\text{where } \tilde{F} = \frac{3}{4} c_x \frac{\mathbf{r}_v \Delta w}{\mathbf{r}_d D_d}; \quad c_x = f(\text{Re}_d); \quad \text{Re}_d = D_d \Delta w \mathbf{r}_v / \mathbf{m}_v.$$

From momentum equation for evaporating wall fluid layer of varying mass we have

$$\frac{dw_{wl}}{d\mathbf{j}} = \left(\frac{(\overline{w}_d \mathbf{j} - \overline{w}_{wl})}{b_b} \frac{dG_{fd}}{d\mathbf{j}} - \mathbf{d}_{wl} \frac{dp}{d\mathbf{j}} - \mathbf{t}_{wl} R_b \right) / (\overline{w} \mathbf{d} r)_{wl},$$

where R_b -radius of concave blade surface. It is assumed in calculations that droplet is considered as fallen one (subscript "fd") if its trajectory crosses the wall layer surface and the

layer gets a mass of droplets per second $dG_{fd} = p n_c \mathbf{r}_d D_d^3 d\mathbf{j} / 6$, where n_c - droplet mass flux per cell. It is assumed also that mass of all droplets crossing given cell is united in a single droplet of the same (given) size. From continuity equation for wall layer (subscript "wl") we find

$$\frac{d\mathbf{d}_{wl}}{d\mathbf{j}} = \left[\frac{1}{b_b} \frac{dG_{fd}}{d\mathbf{j}} - \Delta j_{wl-v} (R_b - \mathbf{d}_{wl}) \right] / \left(\bar{w} \mathbf{r}_{wl} \right) - \frac{\mathbf{d}_{wl}}{w_{wl}} \frac{d\bar{w}_{wl}}{d\mathbf{j}}.$$

Having written an equation of heat account between droplet and vapor flow, we get

$$\frac{dT_d}{d\mathbf{j}} = - \frac{6r}{\mathbf{r}_d D_d c_{pd} w_{dj}} (\mathbf{a}_{d-v} (T_d - T_v) + \tilde{r} \Delta j_{d-v}).$$

A derivative $dT_{wl}/d\mathbf{j}$ can be found from energy equation and mass balance of wall layer:

$$\begin{aligned} \frac{dT_{wl}}{d\mathbf{j}} = & \left[\left(\frac{i_d^* - i_{wl}^*}{d\mathbf{j}} \right) G_{fd} - \left(\left(i_v^* (T_{wl}) - i_{wl}^* \right) j_{wl-v} - \right. \right. \\ & \left. \left(i_v^* (T_v) - i_{wl}^* \right) j_{v-wl} + \mathbf{a}_{wl-v} (T_{wl} - T_v) \right) \times \\ & \times (R_b - \mathbf{d}_{wl}) b_b \right] / \left(\bar{w}_{wl} G_{wl} \right) - \frac{\bar{w}_{wl}}{c_{pw wl}} \frac{d\bar{w}_{wl}}{d\mathbf{j}}. \end{aligned}$$

The droplet concentration in a cell n_c is defined from expression $n_V = n_c dl / (w_d r d\mathbf{j} dr)$, where dl is droplet trajectory length inside a cell. The above system of equations is closed and permits to find w_{vj} , w_{dj} , w_{dr} , p , D_d , T_d , \bar{w}_{wl} , \mathbf{d}_{wl} , T_{wl} along the channel, Barilovich *et al.* (1996). The HST stage capacity at working wheel rim can be found from formula

$$N_{HST} = [(G_v w_{vu} + G_d w_{du})_{inlet} - (G_v w_{vu} + G_d w_{du} + G_{wl} \bar{w}_{wl})_{outlet}] z_u,$$

where z - number of moving blades. The system of differential equations is solved by Runge-Kutta-Feldberg method. The physical properties of water and vapor is approximated by spline functions of pressure.

The calculations have shown that the wall layer slows down in initial zone of concave blade surface. Then its velocity begins to grow due to momentum quantity bringing by droplet flux. After that layer velocity decreases again because frictional forces begin to prevail. An influence of blade pitch and profile on HST efficiency has been determined. The moving blades must have sharp edges, long entry and short exit parts.

The results of experiments obtained during tests of model of axial active single-row HST-100 at partial admission degree of 0.15 and outlet into atmosphere are shown at Fig.4.5. At full admission of high-moistened vapor to moving blades the design turbine capacity would be 65...107 kW.

In investigations of single block of nozzles of HST-100 a value $j_n = 0.74$ was obtained which corresponds to design HST capacity of 82.5 kW and relative internal blade efficiency $h_{ou} = 0.391$ at $p_o^* = 0.6$ MPa, $T_o^* = 427$ K and $G = 14.53$ kg/s. A usage of high-effective nozzles with $j_n = 0.85$ would permit to get $N = 115.9$ kW and $h_{ou} = 0.549$.

5. ON CALCULATION OF PELTON TURBINE WORKING AT FLASHING FLOW

The theory of hydraulic Pelton turbines (PT) working at "cold" flows is well worked out and presented in a number of fundamental works like Edel (1980). However, it is only partially applicable for predicting of Pelton HST (Trusov *et al.* (1995), Barilovich *et al.*, (1997)).

As the condenser-mixer is an obligatory element of such turbines ensuring a required relation between jet diameter and scoop size of working wheel, it is necessary to consider the basics of calculation of mixing camera. Let's assume that cold and hot droplets are evenly distributed in dry saturated vapor at entry to MC but the flow has no thermal and mechanical equilibrium. Under its motion along z and presence of exchange processes the flow will move over to equilibrium condition. This transition determines the length of MC. As the flow is high-speed, it may be expected that wall fluid film thickness is very small and may be neglected. The system of equations below permits to execute calculation of MC in one-dimensional approach.

$$\frac{dc_{cd}}{dz} = - \frac{1}{c_{cd} \mathbf{r}_{cd}} \frac{dp}{dz} + \frac{6 D_{cd}^*}{\mathbf{p} D_{cd}^3 c_{cd} \mathbf{r}_{cd}} + \frac{(c_v - c_{cd})}{G_{cd}} \frac{dG_{cond}}{dz},$$

where $dG_{cond} = j_{v-cd} \mathbf{p} D_{cd}^2 n_{Vcd} F_{mc} dz$; j_{v-cd} - specific flow of vapor condensing on cold droplets;

$$D_{cd}^* = c_x \mathbf{p} D_{cd}^2 \mathbf{r}'' (c_v - c_{cd}) |c_v - c_{cd}| / 8 - \text{resistance force of single droplet};$$

$$\frac{dc_{hd}}{dz} = - \frac{1}{c_{hd} \mathbf{r}_{hd}} \frac{dp}{dz} + \frac{6 D_{hd}^*}{\mathbf{p} D_{hd}^3 c_{hd} \mathbf{r}_{hd}};$$

$$\begin{aligned} \frac{dc_v}{dz} = & \left(- f_v \frac{dp}{dz} - \mathbf{t}_w \mathbf{p} D_{mc} - \frac{6 D_{cd}^* G_{cd}}{\mathbf{p} D_{cd}^3 c_{cd} \mathbf{r}_{cd}} - \right. \\ & \left. - \frac{6 D_{hd}^* G_{hd}}{\mathbf{p} D_{hd}^3 c_{hd} \mathbf{r}_{hd}} - (c_v - c_{hd}) \frac{dG_{vap}}{dx} \right) / G_v; \end{aligned}$$

$$\begin{aligned} \frac{dp}{dz} = & \frac{c_v}{(\Delta_s - 1) f_v} \left\{ - \frac{F_{mc}}{c_v} \left[D_{hd}^* n_{Vhd} \left(\frac{c_v^2 \mathbf{r}''}{c_{hd}^2 \mathbf{r}_{hd}} - 1 \right) + \right. \right. \\ & \left. \left. + D_{cd}^* n_{Vcd} \left(\frac{c_v^2 \mathbf{r}''}{c_{cd}^2 \mathbf{r}_{cd}} - 1 \right) \right] - \right\} \end{aligned}$$

$$\begin{aligned} & - \mathbf{p} F_{mc} \left[\left(\frac{c_v \mathbf{r}''}{c_{hd} \mathbf{r}_{hd}} - \frac{c_v - c_{hd}}{c_v} - 1 \right) D_{hd}^2 n_{Vhd} j_{hd-v} + \right. \\ & \left. + \left(\frac{c_v \mathbf{r}''}{c_{cd} \mathbf{r}_{cd}} (c_v - c_{cd}) - \frac{c_v \mathbf{r}''}{c_{cd} \mathbf{r}_{cd}} + 1 \right) D_{cd}^2 n_{Vcd} j_{v-cd} \right] - \\ & - c_v \mathbf{r}'' \frac{dF_{mc}}{dz} + \frac{\mathbf{t}_w \mathbf{p} D_{mc}}{c_v} \left. \right\}; \end{aligned}$$

$$\begin{aligned}
\Delta_s &= \frac{c_v^2}{dp/d\mathbf{r}''} - \frac{G_{hd}}{G_v} \left(\frac{c_v}{c_{hd}} \right)^3 \left(\frac{\mathbf{r}''}{\mathbf{r}_{hd}} \right)^2 - \frac{G_{cd}}{G_v} \left(\frac{c_v}{c_{cd}} \right)^3 \left(\frac{\mathbf{r}''}{\mathbf{r}_{cd}} \right)^2; \\
T_{hd} &= \frac{1}{c_{phd} G_{hd}} \left[I_{mix0}^* - G_v \left(i'' + \frac{c_v^2}{2} \right) - \right. \\
&\quad \left. - G_{cd} \left(i_{cd} + \frac{c_{cd}^2}{2} \right) \right] - \frac{c_{hd}^2}{2c_{phd}} + 273; \\
\frac{dT_{cd}}{dz} &= \frac{1}{c_{pcd}} \left\{ \left[\left(i''^* (T_v) - i_{cd}^* \right) j_{v-cd} - \left(i''^* (T_{cd}) - i_{cd}^* \right) j_{cd-v} \right] + \right. \\
&\quad \left. + \mathbf{a}_{v-cd} (T_v - T_{cd}) \right] \frac{6}{(c \mathbf{r} D)_{cd}} - c_{cd} \frac{dc_{cd}}{dz} \right\}.
\end{aligned}$$

In order to minimize shock losses in MC pumps with $p = p_p/p_e = 25 \dots 50$ should be used in cold water line.

6. RESULTS OF EXPERIENCED STUDIES

This section presents some experimental results which are necessary for HST calculations and determining of external characteristics of investigated model.

The critical mass flow through the nozzle described in Barilovich (1993) is defined by empirical expression obtained for the nozzles with steam generating lattices working at overheated water:

$$\frac{G_{cr,a}}{F_l} = 1.3434 p_0^{*0.751} \left(\Delta t_u / t_s (p_0^*) \right)^{0.372} (l/d)_l^{-0.028},$$

where $G_{cr,a}$ -actual hot water flow through nozzle at critical regime; F_l -steam generating lattice passage area; p_0^*, t_0^* -hot water pressure and temp. at nozzle entry; $\Delta t_u = t_s (p_0^*) - t_0^*$ -underheating of water to saturation temperature; $(l/d)_l$ -relative length of lattice holes. The value of friction coefficient between high-speed fluid wall layer and wall $c_{fr,w} = f(\text{Re}_{flm})$ is needed in gas-dynamic calculations of HST foil lattice. Known data at co-current moving of vapor and fluid film are obtained at low mean film velocity \bar{w}_{flm} ($\text{Re}_{flm} = \bar{w}_{flm} d / \mathbf{n}_f \leq 800$). Experiences for determining of $c_{fr,w}$ were carried out in open rectangular duct of 0.014 m width and 1 m length. At entry to the duct a Laval nozzle working at overheated water was mounted. The axis of nozzle was inclined at angle of 15° to duct longitudinal axis. The dynamic pressure measurements were made by Prandtl microtube (see Fig.6). The tube width was 3 mm, and thickness 0.4 mm. It was moved across the duct by the precision support with accuracy 0.01 mm. Processing experienced data in criterial form gives

$$c_{fr,w} = 0.577 \cdot 10^{-9} \text{Re}_{flm}^{0.981}, \quad 5 \cdot 10^6 \leq \text{Re}_{flm} \leq 11 \cdot 10^6,$$

$\text{Re}_{flm} = (\bar{w}_{flm} z) / \mathbf{n}_{flm}$. The same in two-parametric form $c_{fr,w} = f(\text{Re}_{flm}, \text{Eu})$ leads to

$$c_{fr,w} = 0.46 \cdot 10^{-13} \text{Re}_{flm}^{1.62} \text{Eu}^{0.47}$$

at $\text{Eu} = (p / \mathbf{r} c^2)_{z=0} = 0.36 \dots 0.79$. In this case Euler number, being a defining criteria, characterizes kinetic energy of flow at nozzle exit. Mean value of $\bar{c}_{fr,w}$ at distance $z=0.115$ m is equal to $5.29 \cdot 10^{-3}$. It must be noticed that Wallis (1972) recommends $\bar{c}_{fr,w} = 0.005$ as a first approach at turbulent regime of film flow.

CONCLUSION

The data presented show that geothermal hydrosteam electric stations of new generation should include hydrosteam turbines, which greatly raise the installation efficiency under low dryness degree of inlet geothermal mixture.

REFERENCES

Barilovich, V.A. (1982). On using of hydrosteam turbines in geothermal energetics. *Physical processes in mining industry*, Vol.12, pp. 97-105, Leningrad.

Barilovich, V.A. (1993). Hydrosteam turbines and their application in geothermal energetics, *Heat energetics*, No.3, pp. 35-38.

Barilovich, V.A., Miroshnikov, Y.A., Starikov, V.I. and Remzhan, S.Y. (1987). Increasing of efficiency of flash flow nozzles. *Izvestia vuzov. Energetics*, No.5, pp.56-60.

Barilovich, V.A., Smirnov, Y.A. (1996). The design of axial hydrosteam turbines. In: *Non-traditional energetics: resources, technics, economics, ecology*, St.Petersburg, SPbSTU, pp.112-117.

Barilovich, V.A., Smirnov, Y.A. (1997). On calculation of flash-water Pelton turbines. *Proceedings of SPbSTU*, No.465, pp.96-105.

Barilovich, V.A., Smirnov, Y.A. (1998). Thermodynamic analysis of geothermal heat power stations with hydrosteam turbines. *Promyshlennaya teplotechnika*, Vol.20, No.2, pp.37-42.

Barilovich, V.A., Smirnov, Y.A., and Starikov, V.I. (1985). On heat efficiency of geothermal electric stations, *Heat energetics*, No.11, pp. 54-56.

Edel, Y.U. (1980). *Scoop hydroturbines*. Machinostroenie, Leningrad, 228 p.

Frenzl O. (1956) Strömung verdampfenden Wassers in Düsse. *Maschinenbau und Wärmeleistung*, No.1, p.11, No.2, p.45.

Trusov, V. and Kabakov, V. (1995). Geothermal power plants on the basis of application of total flow energy conversion. In: *Proceedings of WGC, Florence, Italy, 18-31 May*, Vol.3, Sect.9, pp.2119-2124.

Wallis, G.B. (1972). *One-dimensional two-phase flow*. McGraw Hill, N.Y. 440 p.

Zysin, V.A. (Ed.), (1976). *Flashing adiabatic flows*. Atomizdat, Moscow. 152 p.

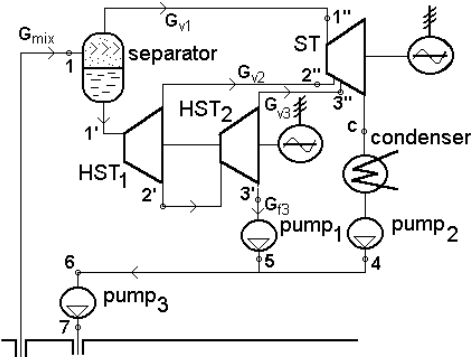


Figure 1. Scheme with two HST

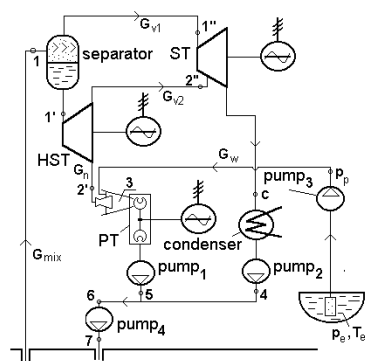
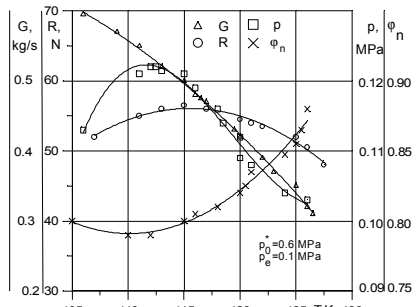
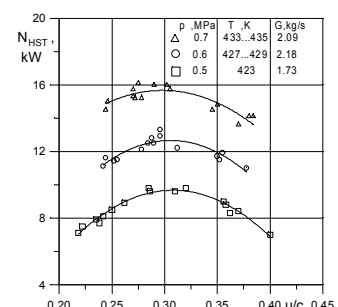
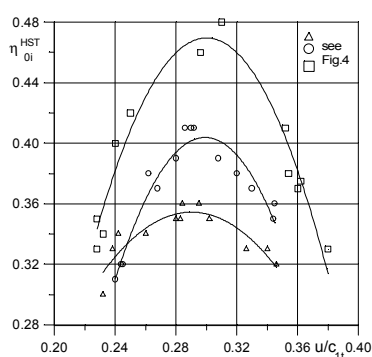
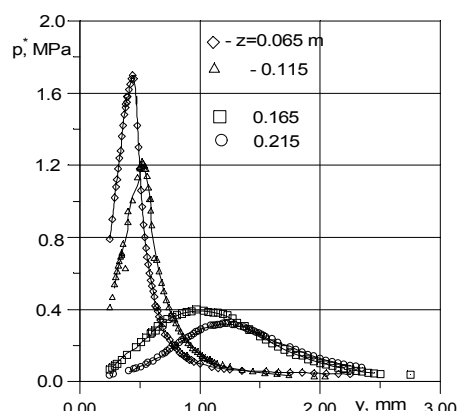


Figure 2. Scheme with HST and Pelton turbine

Table 1. Scheme No.1 with two HST, $G_{\text{mix}}=166.7 \text{ kg/s}$; $h_{\text{HST1}}=0.42$; $h_{\text{HST2}}=0.42$; $h_{\text{ST}}=0.7$; $h_p=0.72$

t_{mix}	x	N_{ST}	N_{HST1}	N_{HST2}	N_{GEO}	ΔN	t_2/t_{mix}	t_3/t_{mix}	h_i	h_{ex}
C		MW	MW	MW	MW	%				
160	0.050	9.278	0.765	0.523	10.426	17.19	0.706	0.463	0.127	0.426
	0.150	16.197	0.571	0.467	17.095	8.30	0.731	0.488	0.147	0.468
	0.250	23.064	0.504	0.370	23.798	4.94	0.731	0.500	0.156	0.490
170	0.050	10.444	0.890	0.684	11.835	18.16	0.700	0.435	0.132	0.441
	0.150	17.716	0.734	0.557	18.825	9.10	0.712	0.459	0.153	0.481
	0.250	24.947	0.595	0.446	25.806	5.39	0.724	0.482	0.164	0.501
180	0.050	11.695	1.101	0.730	13.293	18.77	0.683	0.422	0.139	0.455
	0.150	19.244	0.915	0.653	20.580	9.94	0.694	0.433	0.158	0.492
	0.250	26.794	0.749	0.527	27.838	6.02	0.706	0.456	0.170	0.512
190	0.050	12.961	1.333	0.843	14.843	19.58	0.668	0.400	0.144	0.469
	0.150	20.785	1.116	0.754	22.361	10.69	0.679	0.411	0.164	0.503
	0.250	28.615	0.920	0.613	29.854	6.61	0.689	0.432	0.176	0.521

Figure 3. Dependence of mass flow G , traction R , exit pressure p , velocity coeff. j_n on entry temperature T Figure 4. HST capacity vs u/c_{lt} Figure 5. HST relative internal efficiency vs u/c_{lt} Figure 6. Pressure across fluid wall layer at different distances z from entry to duct